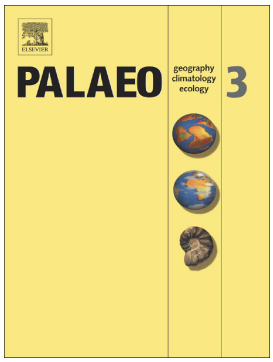

Coniacian-Campanian magnetostratigraphy of the Marambio Group: The Santonian-Campanian boundary in the Antarctic Peninsula and the complete Upper Cretaceous – Lowermost Paleogene chronostratigraphical framework for the James Ross Basin

Florencia N. Milanese, Eduardo B. Olivero, Sarah P. Slotznick, Thomas S. Tobin, María E. Raffi, Steven M. Skinner, Joseph L. Kirschvink, Augusto E. Rapalini

PII: S0031-0182(20)30316-3

DOI: https://doi.org/10.1016/j.palaeo.2020.109871

Reference: PALAEO 109871

To appear in: *Palaeogeography, Palaeoclimatology, Palaeoecology*

Received date: 21 January 2020

Revised date: 11 May 2020

Accepted date: 11 June 2020

Please cite this article as: F.N. Milanese, E.B. Olivero, S.P. Slotznick, et al., Coniacian-Campanian magnetostratigraphy of the Marambio Group: The Santonian-Campanian boundary in the Antarctic Peninsula and the complete Upper Cretaceous – Lowermost Paleogene chronostratigraphical framework for the James Ross Basin, *Palaeogeography, Palaeoclimatology, Palaeoecology* (2019), https://doi.org/10.1016/j.palaeo.2020.109871

Coniacian-Campanian magnetostratigraphy of the Marambio Group: the Santonian-Campanian boundary in the Antarctic Peninsula and the complete Upper Cretaceous – lowermost Paleogene chronostratigraphical framework for the James Ross Basin

Florencia N. Milanese[1,*] fnmilanese@gl.fcen.uba.ar, Eduardo B. Olivero[2], Sarah P. Slotznick[3], Thomas S. Tobin[4], María E. Raffi[5], Steven M. Skinner[6], Joseph L. Kirschvink[7,8], Augusto E. Rapalini[1]

[1]Instituto de Geociencias Básicas, Aplicadas y Ambientales de Buenos Aires (IGeBA), Buenos Aires, Argentina

[2]Centro Austral de Investigaciones Científicas (CADIC-CONICET), Ushuaia, Tierra del Fuego, Argentina

[3]Department of Earth Sciences, Dartmouth College, Hanover, NH, USA

[4]Department of Geological Sciences, University of Alabama, Tuscaloosa, AL, USA

[5]Instituto de Ciencias Polares, Ambiente y Recursos Naturales (ICPA, UNDTF), Ushuaia, Tierra del Fuego, Argentina

[6]Department of Geology, California State University, Sacramento, CA, USA

[7]Division of Geological and Planetary Sciences, California Institute of Technology, Pasadena, CA, USA

*Corresponding author at: Intendente Güiraldes 2160 – C1428EGA – Buenos Aires, Argentina.

Abstract

Recent magnetostratigraphic works from different areas of the James Ross Basin have expanded on chronostratigraphic studies previously based on ammonite, palynomorph and nanoplankton biostratigraphy, and strontium

isotope stratigraphy. Here we present a new magnetostratigraphy of Coniacian through Campanian marine sedimentary rocks from Hidden Lake, Santa Marta and Snow Hill Island Formations, on northwest James Ross Island. A total of 189 paleomagnetic directions were obtained along more than 1500 m of stratigraphic thickness from Brandy Bay to Santa Marta Cove areas, identifying three polarity chrons of the global polarity time scale. The local magnetostratigraphic column starts in the upper part of the Cretaceous Normal Superchron C34N (Coniacian) and ends in Chron C33N (middle Campanian). The correlation between the magnetostratigraphy and the age framework given by ammonite biostratigraphy allowed the assignment of precise ages to particular horizons of the Santa Marta Formation. The newly identified geomagnetic polarity reversals are the oldest identified in the James Ross Basin and include: a) C34N/C33R (84.2 Ma, late Santonian – early Campanian) in the Alpha Member of the Santa Marta Formation and b) C33R/C33N (79.9 Ma, middle Campanian) in the upper Beta Member (Santa Marta Formation). By integrating this new data with previous work, we present a complete Upper Cretaceous – lowermost Paleogene chronostratigraphical framework for the basin, spanning both proximal to distal sedimentary facies of the Marambio Group.

Keywords: Late Cretaceous, ammonites, paleomagnetism, biostatigraphy, Cretaceous Normal Superchron, Coniacian-Santonian boundary

1. Introduction

Located at the northeastern tip of the Antarctic Peninsula (Fig. 1), the James Ross Basin (JRB) contains one of the most complete Upper Cretaceous sections for the Southern Hemisphere (Crame et al., 1991, 1996; Feldmann and Woodbourne, 1988; Olivero, 2012a; Witts et al., 2016). It comprises more than 6 km of marine clastic and volcaniclastic strata, of Barremian to Eocene age. The strata are exposed on James Ross, Snow Hill, Marambio (Seymour), and Vega Islands as well as on other smaller islands of the James Ross archipelago (Fig. 1). An important characteristic of the basin is the abundant and diverse vertebrate, invertebrate, and plant fossil content. It also includes the Cretaceous - Paleogene boundary in the upper Marambio Group on Marambio (Seymour) Island and a possible boundary on Vega Island (Roberts et al., 2014), and is a key element in paleobiogeographic reconstructions of the Southern Hemisphere and global extinction patterns (Barreda *et al.*, 1999; Crame *et al.*, 1996; Iglesias 2016, Petersen *et al.*, 2016; Rolfi and Olivero, 2016; Reguero *et al.*, 2013; Tobin, 2017; Witts *et al.*, 2016).

The stratigraphy of the basin is based mainly on the correlation of isolated sections using sequence stratigraphic principles in combination with biostratigraphy from palynomorphs, ammonites, and nannoplankton, as well as sparse $^{87}Sr/^{86}Sr$ isotopic data (Crame *et al.*, 1999; do Monte Guerra *et al.*, 2015; McArthur *et al.*, 2000; Olivero, 2012a; Olivero *et al.*, 1986). Although the intra-basin correlation of units has been well established, problems of endemism and early extinction of several biostratigraphically important invertebrate groups (notably heteromorph ammonites and inoceramid clams) in Antarctica hamper global correlations (Crame *et al.,* 1996; Francis *et al.,* 2006; McArthur *et al.,*

2000; Olivero, 2012a; Olivero and Medina, 2000; Raffi and Olivero, 2016). To overcome this obstacle, it is necessary to obtain an independent and precise age framework for the Cretaceous JRB infill.

Magnetostratigraphy has been demonstrated as effective in the southeast part of the basin (Milanese et al., 2019a; Montes et al., 2019; Tobin et al., 2012), and here we present new magnetostratigraphic data for the northwest area that encompass the Hidden Lake, Santa Marta, and Snow Hill Island Formations. This study unites the major exposures of the JRB into a common magneto- and bio-stratigraphic framework that can be used to correlate the strata of the Antarctic Peninsula to other regions in Cretaceous and early Cenozoic times.

2. Geologic setting

The James Ross Basin is a back-arc basin developed to the east of the magmatic arc located on the Antarctic Peninsula and its marine Cretaceous infill is divided into two major groups: the Aptian-Coniacian Gustav Group and the Santonian-Danian Marambio Group. Outcrops of the Gustav Group are restricted to the northwest margin of James Ross Island and comprise a coarse–grained, deep marine slope apron system deposited in a normal fault - regulated environment that was located along the present Prince Gustav Channel (Fig. 1). It includes five units, and the upper one, Hidden Lake Formation, represents the first stages of the depositional setting for the development of the shallow-marine deposits of the Marambio Group (Buatois and López Angriman, 1992; Ineson, 1989; Whitham *et al.,* 2006).

The Marambio Group contains more than 3 km of strata that consist mainly of poorly consolidated mudstones, mud-rich sandstones, and occasional coquina

and conglomerate beds, most with abundant fossils. An onshore-offshore trend in deposition is evident in the JRB from the northwest to the southeast, with the center of deposition moving progressively to the southeast during the Late Cretaceous. Olivero (2012a) recognized three stratigraphic sequences within the Marambio Group, facilitating correlations between different formations and members across the basin. Upper Cretaceous stratigraphy of the JRB is summarized in Figure 2.

The new magnetostratigraphic results presented in this paper come from the upper Gustav Group and the proximal facies of the Marambio Group on the Ulu Peninsula of James Ross Island (Figs. 1, 2), which correlate to distal strata located in the southeastern sector of James Ross Island. The stratigraphically lowest samples include the upper half of the Hidden Lake Formation, of the underlying Gustav Group, and Marambio Group samples come from Santa Marta and Snow Hill Island formations. The chronostratigraphic scheme from Figure 2 also summarizes the previous magnetostratigraphic results from the southeast area (Milanese *et al.*, 2019a, 2017; Tobin *et al.*, 2012), together with a compilation of the age constraints published for the Cretaceous of the Ulu Peninsula to the date. Based on inoceramid species assemblages, Crame *et al.* (2006) place the Turonian-Coniacian boundary at the base of the Hidden Lake Formation and the ammonites indicate mainly a Coniacian age (Kennedy *et al.*, 2007). Palynomorphs also support a Coniacian age, with the Coniacian-Santonian boundary probably located near the top of the Hidden Lake Formation (Barreda *et al.*, 1999). On the contrary, $^{87}Sr/^{86}Sr$ studies (McArthur *et al.*, 2000) establish the Coniacian – Santonian boundary at the 150 m level of the Santa Marta Formation and the Santonian – Campanian boundary about

300-350 m below the top of the Santa Marta Formation, *i.e.* below the level with large *Antarcticeramus rabotensis*. According to the Ammonite Assemblages 1 to 6, this unit is assigned to the Santonian – early Campanian (Olivero, 1992).

Hidden Lake Formation (Gustav Group) is restricted to northwest James Ross Island (Figs. 1, 2). It represents the toesets of a substorm-wave base fan delta succession passing laterally and vertically into a basin floor facies association; these deeper water submarine-fan and slope-apron environments are overlain by the shallow-marine-shelf facies of the Santa Marta Formation (Whitham *et al.*, 2006). In the study area, it consists in a fining-upwards intercalation of mudstones, sandstones and conglomerates. Massive or cross-stratified, medium-coarse sandstones bodies are common, as well as heterolithic beds filling slump scars. The invertebrate fauna is composed of abundant marine invertebrates (inoceramids, ammonoids and brachiopods) (Barreda et al., 1999; Kennedy et al., 2007; Medina and Buatois, 1992). Figure S1a (supplementary material) shows a view of the sampled section.

The Santa Marta Formation (Figs. 2, 3) crops out on northwest James Ross Island. Its thickest section spans from Brandy Bay to Santa Marta Cove, reaching ~ 1100 m of sedimentary thickness. The lower Alpha Member is composed of mostly poorly consolidated muddy sandstones and very fine tuffs, and there are also some minor intercalations of hardened coarsening-upward tuff beds with bioturbated mudstones at the top. The upper Alpha Member is characterized by sandy and tuff-rich normally graded and thickening upward beds, covered by laminated mudstones with carbonized plants fragments. The lower Beta Member consists in normally graded tuffs and sandy coarse-grained turbidites, erosively cut by channels filled with resedimented conglomerates and

debris flows. Synsedimentary folds are also relatively common. The upper Beta Member consists in alternated fine and muddy bioturbated sandstones with mudstones rich in plants, trunks and leaves fragments. Figures S1b,c,d,e (supplementary material) show views of the Alpha Member sampled sections.

Exposures of the late Campanian – early Maastrichtian (Milanese et al., 2019a) Snow Hill Island Formation are distributed across the James Ross Basin (Figs. 1, 2), encompassing ~ 1000 m of mostly unconsolidated mudstones and fine sandstones. It is divided in three members at the southeast sector: Hamilton Point, Sanctuary Cliffs, and Karlsen Cliffs Members; and in two members in the northwest sector of the basin: Gamma and Cape Lamb Members. The basal contact with the Santa Marta Formation in the study area is unconformable and marked by a conglomerate containing reworked ammonites. These ammonites constitute the Assemblage 7, that is restricted to the distal part of the basin, which suggests that was eroded from the top of Santa Marta Formation. The data presented here are restricted to the Gamma Member, comprised mostly of unconsolidated sandstones and coquinas. The Ammonite Assemblages 8-1 to 9 are contained in this unit and indicate a late Campanian age. According to the 71.3 Ma age obtained by $^{87}Sr/^{86}Sr$ results from Crame *et al.* (1999), the overlying Cape Lamb Member contains the Campanian Maastrichtian boundary. Figures S1f (supplementary material) shows a view of the sampled section.

For a more detailed description of the lithology and fossil content of the studied units, we refer the reader to Olivero (2012a).

3. Methodology

3.1 Field sampling

Systematic sampling was carried out along thirteen partial sections located on northwest James Ross Island, encompassing levels from the Hidden Lake, Santa Marta, and Snow Hill Island formations (Figs. 3, S1). The strata dip 10-12° to the east-southeast, with minor local variations and small scale normal and reverse faulting. Field observations constrained the stratigraphic correlation between partial sections. Magnetostratigraphic sampling was carried out using a portable gasoline-powered drill. We collected 210 standard paleomagnetic cores (from which 189 characteristic paleomagnetic directions were isolated) oriented *in situ* with sun and magnetic compasses and located precisely within stratigraphy using a Jacob's staff. Each sample corresponds to a discrete stratigraphic level, targeting the better cemented sandstone beds and isolated spherical concretions.

3.2 Paleomagnetic methods

Measurements were carried out on 5.5 cm^3 paleomagnetic specimens at the Paleomagnetics and Biomagnetics laboratory of the California Institute of Technology, using an automatic 3-axis DC-SQUID moment magnetometer system, housed in a magnetically shielded room. The applied demagnetization routine, already proved successful in Marambio Group rocks (Milanese *et al.*, 2019a, 2017; Tobin *et al.*, 2012), started with two low-temperature cycling steps (samples were cooled to 77 K in liquid N_2 in a low field space) to remove viscous magnetizations carried by multidomain magnetite, followed by three low-intensity alternating field (AF) steps (from 2.3 to 6.9 mT) to remove secondary magnetizations acquired during collection and transportation of

samples. The main demagnetization process was thermal, from 80 °C to 575 °C in 10-15 °C steps, with samples being demagnetized in a trickle of N_2 gas above 120 °C to minimize oxidation. At the same laboratory, we measured isothermal remanent magnetization (IRM) acquisition up to 900 mT and AF demagnetization up to 100 mT, backfield acquisition curves up to 900 mT, and anhysteretic remanent magnetization (ARM) acquisition and alternating field (AF) demagnetization curves (AF_{MAX} 100 mT and 10 different continuous fields). Hysteresis loops were collected using a Molspin vibrating sample magnetometer NUVO at the Laboratorio de Paleomagnetismo Daniel A. Valencio of the IGEBA (University of Buenos Aires - CONICET, Argentina).

4. Results

4.1 Magnetic mineralogy

Coercivity values from hysteresis loops (Fig. 4a) are between 8 and 12 mT. Both hysteresis loops and IRM/Backfield curves (Fig. 4b) show that saturation is reached at ~ 300 mT. The coercivity spectra from IRM acquisition and demagnetization (Kruiver *et al.*, 2001) show a normal distribution centered on values between 31 and 39 mT (Fig. 4b). All calculated magnetic parameters from hysteresis loops and IRM/Backfield curves are available in Supplementary Material (Table S1, Figs. S2, S3, S4). Due to moderate coercivity values and saturation fields of ~ 300 mT, we interpret that a ferrimagnetic phase, probably titanomagnetite, is the main magnetic phase in the study rocks. Milanese *et al.* (2017) described detailed rock magnetics analyses on the Rabot Formation samples that successfully eliminated the presence of greigite, confirming that the most likely remanence carrier is within the titanomagnetite series.

Lowrie-Fuller (Lowrie and Fuller, 1971) tests from Figure 4c show that ARM is more resistant to AF demagnetization than IRM, a characteristic behavior of single domain or psuedo-single domain (a.k.a. vortex state) (titano)magnetite. The Day plot (Dunlop, 2002), that is provided in the Supplementary Material (Fig. S5), also indicates that most samples from Hidden Lake and Santa Marta Formations belong to the pseudo-single domain field. This pseudo-single domain range could record a mixture of single-domain (SD) and multi-domain (MD) grains (40-95% MD *e.g.* Dunlop, 2002) or vortex state grains, which have been shown recently to be stable over long time periods (Nagy *et al.*, 2017). Similar conclusions were obtained by Milanese *et al.* (2019a, 2017) and Tobin *et al.* (2012) for approximately equivalent units at the southeast area of the JRB.

4.2 Magnetostratigraphy

A magnetostratigraphic composite column was built for the northwest JRB based on thirteen partial sections. Figure 3 shows their location and stratigraphic correlation. Demagnetization revealed two components in most samples: a viscous remanence eliminated during the first demagnetization steps (low liquid N_2 temperatures, low AF fields and thermal steps below 150 °C) and a high-temperature component interpreted as the characteristic remanent magnetization ChRM with blocking temperatures (T_B) around 450 – 550 °C (Fig. 5). A wide T_B distribution is observed in the demagnetization diagrams, which is characteristic of many sedimentary rocks, where magnetic minerals show a distribution of composition, size, and grain shape that determines a wide range of T_B and coercivities (*e.g.* Dunlop and Ozdemir, 1997). In a few cases, demagnetization diagrams show remaining magnetization above ~ 550 °C (*e.g.* Fig. 5c), which could indicate hematite

presence. However, this could not be confirmed in the rock magnetic analysis, and thermal demagnetization did not exceed 550 °C in any case, due to unstable behaviors observed above those temperatures and produced, most likely, by chemical changes in clay minerals upon heating (Pan *et al.*, 2000). This unstable behavior above 400-500 °C was previously found by Milanese *et al.* (2019a, 2017) and Tobin *et al.* (2012) in the sedimentary successions of the southeast sector of the basin.

From the 189 samples, most paleomagnetic directions were calculated through Principal Component Analysis (PCA; Kirschvink, 1980) and only those with Maximum Angular Deviation (MAD) ≤ 10° were accepted. In 29 samples, mostly those magnetized with reverse polarity directions, the directions were obtained by Great Circle Analyses (McFadden and McElhinny, 1988) and are noted as such in all figures and tables (Table S2, Figs. 7, S6 to S20).

Mean paleomagnetic directions were calculated using PCA components only and are: Dec. 30.5°, Inc. -74.8°, α_{95}=3.8°, n=158 (*in situ)* and Dec. 2.7°, Inc. -71.3°, α_{95}=3.9°, n=158 (stratigraphic). Both normal and reversed directions were noted (Fig. 6), and therefore a reversal test could be performed and resulted in a positive class C reversal test (McFadden and McElhinny, 1990). Due to the nearly homoclinal character of the sampled sections, statistical parameters *in situ* and after tilt correction are virtually identical and any fold-test for the age of the magnetization is indeterminate. However, when computing a paleomagnetic pole from these sections, Milanese *et al.* (2019b) found significant inclination shallowing which is consistent with a primary nature of the characteristic remanence. The calculated paleomagnetic pole coordinates are Lat. -82.7°, Long. 134.2°, A_{95}=6.1°, which is similar to a previous one calculated by

Milanese *et al.* (2019b) for the same area: Lat. -88.7°, Long. 302.2°, A_{95}=5.6°. The previous paleopole was calculated without including Gamma Member directions, the most likely cause of the slight difference. Results are summarized in Table 1.

Paleomagnetic results (declination, inclination, and MAD *vs.* stratigraphic level) of the thirteen partial sections (Fig. 3) of the Upper Cretaceous strata from northwest JRB are shown in Figure 7. Directions are summarized in Table S2 and are shown for each partial sedimentary column independently (Figs. S7 to S20) in the supplementary material.

Figure 8 shows the composite magnetostratigraphy that encompasses over 1,400 m of stratigraphic thickness and it is characterized by three well-defined magnetozones, comprising a transition from normal to reversed and back to normal polarity. We applied the secular variation filter proposed by Vandamme (1994), which considers the Virtual Geomagnetic Poles (VGPs) located at a distance > 80° from the mean paleopole as transitional. Therefore, all VGPs within 10° and -10° paleolatitude were ruled out from polarity interpretation and correlation to the Global Polarity Time Scale from Ogg *et al.* (2016).

Figure 8 shows that the basal *ca.* 400 m record normal polarity directions exclusively, encompassing the upper levels of the Hidden Lake Formation and the lowest *ca*. 150 m of the Alpha Member of the Santa Marta Formation where the first reversal is observed within Ammonite Assemblage 1 of Olivero (2012a). The reversed polarity continues through the overlying 600 m from Assemblage 1 into Assemblage 6, which comprises the middle and upper parts of Alpha Member and lower and middle parts of Beta Member of the Santa Marta Formation. Two short intervals of normal polarity, defined by two samples each,

are observed at near the base and top of this reversed section. The uppermost part of the Beta Member and the lower levels of the Snow Hill Island Formation are characterized by almost entirely normal polarity, spanning Ammonite Assemblages 6 to 8, with the sole exception of two levels near the top of the composite section.

5. Interpretation

The Hidden Lake Formation has previously been assigned to the Coniacian Stage using bio- and chemostratigraphy. The Santa Marta Formation was assigned to the Santonian – early Campanian based on the ammonite content and to the Coniacian – Campanian based on its bivalves and strontium isotope stratigraphy (see Fig. 2 for timescales and citations). Hence, the most logical correlation for the long positive-magnetozone recorded from the ~ 125 m level of Hidden Lake Formation to the middle Alpha Member (~ 550 m level of the composite stratigraphic column, Fig. 8) is with Chron 34N (C34N, the Cretaceous Normal Superchron). This supports the initial idea from Olivero (2012a, 1992) of a Santonian age for the base of Santa Marta Formation and not Coniacian (c.f. McArthur *et al.*, 2000 from chemostratigraphy). As we will further see in this section, C33R chron yields a sedimentary accumulation rate of ~ 15.2 cm/kyr for the Santa Marta Formation. Extrapolating this rate, it would require ~ 1.3 Ma to accumulate the 200 m that separate the C34N/C33R reversion (84.2 Ma) from the Santa Marta/Hidden Lake contact, which places it at least at 85.5 Ma, well above the Coniacian-Santonian limit (86.5 Ma). According to our SARs, this limit should be at the ~ 196 m level of the Hidden Lake Formation, 154 m below the contact between this unit and Santa Marta Formation.

The C34N-C33R boundary was placed at the first reversed polarity samples in the Alpha Member at ~ 550 m stratigraphically, but since we observe another small normal magnetozone, an alternative interpretation could place the reversal at ~ 600 m between the top of Assemblage 1 and the base of Assemblage 2 from Olivero (2012, 1992).

Predominantly reversed polarities, interpreted as C33R, extend from ~625 m to ~ 1175 m within upper Beta Member, spanning biostratigraphic Assemblage 2 through the middle of Assemblage 6 (Fig. 8). However, there are two levels of normal polarity intercalated within this reverse interval that do not correlate with the generally accepted global polarity time scales (*e.g.* Ogg *et al.* 2016). The reversal to C33N (found at ~1175 m) has previously been identified in Ammonite Assemblage 6 in the southeast sector of the basin, particularly in the Rabot Formation (Milanese *et al.*, 2019a, 2017). Keating and Herrero-Bervera (1984), Fry *et al.* (1985), Hambach and Krumsiek (1991) and Montgomery *et al.* (1998) have reported the presence of frequent polarity reversals in C33R, considering them as simple events or cryptochrons (<30 ka). Hambach and Krumsiek (1991) have even proposed a “mixed polarity” interval in middle levels of C33R. Due to the slightly higher MAD values and great circle - defined reverse directions that appear in upper Alpha and Beta members (Fig. S6) that could indicate overlapping T_B from magnetic components, we conservatively interpret these three normal intervals/levels as the product of ineffective demagnetization to isolate the ChRM.

Ammonite Assemblages 2 to 6 from Olivero (2012a) support an early Campanian age in the two-part division of the period. The correlation of this interval with C33R allows us to estimate a mean sedimentary accumulation rate

of ~ 15.2 cm/kyr (652 m in 4.3 Myr) for most of the Santa Marta Formation. This value is in accordance with those established by Einsele (2013) for delta environments such as that of Santa Marta Formation, and with previous rates obtained for the Marambio Group at southeast JRB varying from 10 – 20 cm/kyr (Montes et al., 2019; Tobin et al., 2012) to 9 – 50 cm/kyr (Milanese *et al.*, 2019a), at different stratigraphic levels.

The transition to C33N is interpreted to be at the top of Beta Member (~ 1175 m level), at the base of Assemblage 6 (*Karapadites*, *Natalites* spp. *Group 2*). The succeeding Ammonite Assemblage 7 is missing at the Brandy Bay-Santa Marta Cove section. However, the conglomerate at the base of the Gamma Member includes reworked basal middle Campanian ammonites typical of the Ammonite Assemblage 7, such as *Baculites subanceps* (Matsumoto and Obata), *Metaplacenticeras subtilistriatum* (Jimbo) and *Hoplitoplacenticeras* sp. (Olivero, 2012b, 1992).

Above ~ 1175 m, polarities are almost exclusively normal, except for two isolated levels, and thus we interpret the entire Gamma Member as correlating with C33N. It is unclear how much of the chron/time is recorded in this unit since we are not sure where the top of C33N is. Connection with absolute time is additionally difficult as these outcrops are unconformably separated from the Santa Marta Formation and have a reduced thickness (~ 400 m) of the Snow Hill Island Formation, compared with the at least 1000 m of sedimentary thickness in southeast JRB (Fig. 9).

Chrons 33 through 29 have previously been identified in the southeast sector of the JRB, where Campanian – Maastrichtian distal facies are thicker than in the northwest area. The magnetostratigraphy encompassing from C33R to

C29R was obtained by Milanese *et al.* (2017), Milanese *et al.* (2019a) and Tobin *et al.* (2012) from sections on southeast James Ross Island, Snow Hill Island, and Seymour (Marambio) Island (Figs. 1, 2).

Figure 9 integrates the results from the present work and all previous magnetostratigraphic sections obtained in the Upper Cretaceous units of the JRB. The intra-basinal correlation on this figure is based on C33R/C33N limit.

Although the marker for the Santonian-Campanian boundary is still under debate, the C34N/C33R reversal, dated in 84.2 Ma, is one of the two candidates to define it and it is the one adopted by our reference time scale (Ogg *et al.*, 2016). It occurs within the Alpha Member of the Santa Marta Formation, and almost all of the stratigraphy of this formation was deposited during the C33R chron. The boundary between C33R and C33N is found ~ 100 m below the unconformity that separates the Santa Marta from the Snow Hill Island Formation. According to ammonite biostratigraphy from Olivero (2012, 1992), the Rabot Formation, exposed in the southeast of the JRB, should be correlative with the upper levels of the Beta Member of the Santa Marta Formation, and magnetostratigraphic results confirm this correlation. In the proximal northwestern section, the C33R-C33N reversal occurs in the middle Assemblage 6, whereas in the more distal Rabot Formation in southeast JRB, the C33R-C33N transition occurs very close to the top of Assemblage 6, about 10 m below Assemblage 7.

The stratigraphic thickness of the Snow Hill Island Formation in the northwest area is significantly thinner than in the southeast area (200 *vs.* 800 m, approximately). The absence of Ammonite Assemblage 7 in the northwest suggests an erosional or depositional hiatus. However, the almost exclusive

normal polarity of stratigraphic levels corresponding to Ammonite Assemblages 8-1 and 8-2 found in this area implies a correlation with C33N and stratigraphic levels corresponding to the Hamilton Point Member (base of the Snow Hill Island Formation). The C33N-C32R reversal has been interpreted to be in the upper Hamilton Point Member in prior analyses (Milanese *et al.*, 2019a, Fig. 9). The reverse subchrons(?) of C32 were not found with certainty in the northwest exposures, which suggests that the uppermost studied levels of the Snow Hill Island Formation in this region do not reach the uppermost Campanian. However, this apparent lack of record could due to the reduced thickness of the Snow Hill Island Formation in western James Ross Basin.

Sequence boundaries from Figure 9 delimitate three major transgressive-regressive cycles defined by Olivero (2012a) and Olivero and Medina (2000), in which three abrupt sea level falls are inferred: the first one at the base of the Snow Hill Island Formation, the second at the base of the forced-regression sandstones of the Haslum Crag Formation, and the third at the base of the López de Bertodano Formation (Fig. 10). Sedimentary accumulation rates (SAR) were calculated based on Figure 9 results and are represented in Figure 10, where we defined four linear segments. C33R determinates the first interval in the Santa Marta Formation at the northwest area, with an average SAR of ~ 15.2 cm/kyr. C33N plus C32 Chrons have yielded values of ~ 9.5 cm/kyr for the upper part of Rabot Formation and the Hamilton Point Member in the southeast area of the basin. Although it is reasonable that off shore muddy facies present lower SARs than those of ~ 15.2 cm/kyr obtained for the proximal Santa Marta Formation, these units are not exactly synchronous and any comparison should be considered carefully. The third segment shows a ~ 50.9 cm/kyr SAR

calculated from the upper part of Snow Hill Island Formation, the Haslum Crag Formation and the lower half of López de Bertodano Formation (Fig. 9). This SAR increase has been related to the paleoenvironments interpreted for those units by Olivero et al. (2008), that include prograding deltaic lobes, subtidal channels developed during a forced regression, and estuarine environments. These authors propose that this great sediment thickness should be related to tectonic processes that ended, in the early Maastrichtian, when a quiet stage in the basin tectonics ocurred. The Fuegian Andes, which were in probable crustal continuity with the Antarctic Peninsula by late Cretaceous (Gao et al., 2018; Milanese et al., 2019b; Poblete et al., 2016), record the inception of an orogenic phase of uplift with crustal stacking and shortening in the latest Cretaceous (Torres Carbonell *et al*., 2014). This produced the development and uplift of the Fuegian thin-skinned orogen roughly dated in between 70 and 60 Ma (Klepeis and Austin, 1997; Wilson, 1991) coeval with the pulse of high SAR values in the JRB. The SAR returns to much lower values of ~ 13.9 cm/kyr, in the last segment of the curve (Figure 10), normal values for a transgressive platform environment, as the one interpreted for the deposits of the López de Bertodano Formation (Olivero, 2012a).

Our chronostratigraphic framework (Fig. 11), partially supports the Santonian-Campanian boundary previously proposed by ammonite assemblages, since we placed it stratigraphically higher within Santa Marta Formation. As a result of sedimentary accumulation rates calculation, we infer the location of the Coniacian-Santonian boundary at ~ 196 m level of the Hidden Lake Formation. Although previously reported by Milanese et al. (2019a), it is worth noting the Campanian-Maastrichtian boundary at the base of

Sanctuary Cliffs Member, below the stratigraphic positions proposed by both inoceramids and Sr stratigraphy, and ammonites biostratigraphy.

6. Conclusions

We carried out a detailed magnetostratigraphic study of the Upper Cretaceous Marambio Group exposed in the northwest sector of the JRB. Our sampling encompassed the Hidden Lake (corresponding to the upper levels of the Gustav Group), Santa Marta and Snow Hill Island Formations, covering over 1500 m of relatively continuous sedimentary thickness.

Two geomagnetic polarity reversals were identified and the unambiguous determination of C34N/C33R and C33R/C33N boundaries allowed the determination of precise ages for ammonite assemblages used as biostratigraphic markers in the region: a) 84.2 Ma (Santonian – Campanian boundary) within Ammonite Assemblage 1 *Baculites* cf. *kirki*, at lower levels of the Santa Marta Formation and b) 79.9 Ma (middle Campanian) within Ammonite Assemblage 6 *Karapadites-Natalites* spp. Group 2, at the top of Santa Marta Formation.

This correlation also permits to estimate a sedimentary accumulation rate of ~ 15.2 cm/kyr, which agrees with expected values for delta environments such as that of Santa Marta Formation, and with previous rates obtained for the Marambio Group at southeast JRB.

From the analysis of sedimentary accumulation rates, we infer the position of the Coniacian-Santonian boundary at the ~ 196 m level of the Hidden Lake Formation.

Our results, together with previous work on the distal sedimentary facies of the Marambio Group located at the southeast area of the basin, allow for an

independent correlation of deposits from the proximal and distal areas of the basin which previously was based almost exclusively on ammonite assemblages and Sr isotopes studies. It constitutes the first complete geochronological framework for Marambio Group, the Upper Cretaceous infill of the James Ross Basin.

Acknowledgments

To the Instituto Antártico Argentino and the NSF Office of Polar Programs (Grants OPP-0739541 to J. Kirschvink and OPP-0739432 to P. Ward and E. Steig) for the logistic support during the Antarctic field seasons, and the NSF Office of Polar Programs for support of the laboratory work at Caltech (Grant #1341729 to JLK). Grants from ANPCyT (PICTO 2010-0114) and UNTdF PID-A1 to E. Olivero, and Universidad de Buenos Aires (UBACyT 20020130100465BA) to A. Rapalini provided additional support for this research. To Matías Nasselli for the rock magnetics analyses. Special thanks are due to Matías Vaca, Alvar Sobral, Hang Yu, Lewis Ward, Peter Ward, Eric Steig, Nick Swanson-Hysell, David J. Smith, Tomás Wagener, Tomaso Bontognali, Magalia Bonifacie, Lauren Edgar, Shane Schoepher, and Kelly Hillbun for their help during field work. By last, we would like to thank to Elisabet Beamud and to an anonymous reviewer, whose comments and suggestions helped us to improve the first version of this manuscript.

Declaration of interests

The authors declare that they have no known competing financial interests or personal relationships that could have appeared to influence the work reported in this paper.

References

Barreda, V.D., Palamarczuk, S., Medina, F.A., 1999. Palinología de la Formación Hidden Lake (Coniaciano-Santoniano), isla James Ross, Antártida. Revista Española de Micropaleontología 31, 53–72.

Buatois, L.A., López Angriman, A.O., 1992. Evolución de sistemas deposicionales en el Cretácico del Grupo Gustav, Isla James Ross, Antártida, in: Rinaldi, C.A. (Ed.), Geología de La Isla James Ross de La Isla James Ross. Instituto Antártico Argentino, Buenos Aires, pp. 263–297.

Crame, J.A., Pirrie, D., Riding, J.B., Thomson, M.R.A., 1991. Campanian-Maastrichtian (Cretaceous) stratigraphy of the James Ross Island area, Antarctica. Journal of the Geological Society 148, 1125–1140. doi:10.1144/gsjgs.148.6.1125

Crame, J.A., Lomas, S.A., Pirrie, D., Luther, A., 1996. Late Cretaceous extinction patterns in Antarctica. Journal of the Geological Society 153, 503–506. doi:10.1144/gsjgs.153.4.0503

Crame, J.A., McArthur, J.M.M., Pirrie, D., Riding, J.B., 1999. Strontium isotope correlation of the basal Maastrichtian Stage in Antarctica to the European and US biostratigraphic schemes. Journal of the Geological Society 156, 957–964. doi:10.1144/gsjgs.156.5.0957

Crame, J.A., Pirrie, D., Riding, J.B., 2006. Mid-Cretaceous stratigraphy of the James Ross Basin, Antarctica. Geological Society, London, Special Publications 258, 7–19. doi:10.1144/GSL.SP.2006.258.01.02

do Monte Guerra, R., Concheyro, A., Lees, J., Fauth, G., de Araujo Carvalho,

M., Rodriguez Cabral Ramos, R., 2015. Calcareous nannofossils from the Santa Marta Formation (Upper Cretaceous), northern James Ross Island, Antarctic Peninsula. Cretaceous Research 56, 550–562. doi:http://dx.doi.org/10.1016/j.cretres.2015.06.009

Dunlop, D.J., 2002. Theory and application of the Day plot (Mrs/Ms versus Hcr/Hc) 1. Theoretical curves and tests using titanomagnetite data. Journal of Geophysical Research 107, 1–22. doi:10.1029/2001JB000486

Dunlop, D.J., Ozdemir, 1997. Rock magnetism: fundamentals and frontiers. Cambrigde University Press, New York.

Einsele, G., 2013. Sedimentary basins: evolution, facies, and sediment budget. Springer Science & Business Media. 791 pp.

Feldmann, R.M., Woodburne, M.O., 1988. Geology and paleontology of Seymour Island, Antarctic Peninsula. The Geological Society of America Memoirs 169.

Francis, J.E., Crame, J.A., Pirrie, D., 2006. Cretaceous-Tertiary high-latitude palaeoenvironments, James Ross Basin, Antarctica: introduction. Geological Society of London, Special Publications 258, 1–5.

Fry, G., Bottler, D.J., Lund, P.S., 1985. Magnetostratigraphy of displaced Upper Cretaceous strata in southern California. Geology 13, 648–651.

Gao, L., Zhao, Y., Yang, Z., Liu, J., Liu, X., Zhang, S.-H., Pei, J., 2018. New paleomagnetic and 40Ar/39Ar geochronological results for the South Shetland Islands, West Antarctica, and their tectonic implications. Journal

of Geophysical Research: Solid Earth 123, 4–30. doi:10.1002/2017JB014677

Hambach, U., Krumsiek, K., 1991. Magnetostratigraphie im Santon und Campan des Münsterländer Kreidebeckens. Facies 24, 113.

Iglesias, A., 2016. New Upper Cretaceous (Campanian) Flora from James Ross Island, Antarctica. Ameghiniana 53. doi:10.5710/AMGH.17.02.2016.2930

Ineson, J.R., 1989. Coarse-grained submarine fan and slope apron deposits in a Cretaceous back-arc basin, Antarctica. Sedimentology 36, 793–819. doi:10.1111/j.1365-3091.1989.tb01747.x

Keating, B.H., Herrero-Bervera, E., 1984. Magnetostratigraphy of Cretaceous and early Cenozoic sediments of Deep Sea Drilling Project Site 530, Angola Basin, in: Hay, W.W., Sibuet, J.C. (Eds.), Initial Reports DSDP. pp. 1211–1218.

Kennedy, W.J., Crame, J.A., Bengtson, P., Thomson, M.R.A., 2007. Coniacian ammonites from James Ross Island, Antarctica. Cretaceous Research 28, 509–531. doi:10.1016/j.cretres.2006.08.006

Kirschvink, J.L., 1980. The least-squares line and plane and the analysis of palaeomagnetic data. Geophysical Journal of the Royal Astronomical Society 62, 699–718.

Klepeis, K.A., Austin, J.A.J., 1997. Contrasting styles of superposed deformation in the southernmost Andes. Tectonics 16, 755–776.

Kruiver, P.P., Dekkers, M.J., Heslop, D., 2001. Quantification of magnetic

coercivity components by the analysis of acquisition curves of isothermal remanent magnetisation. Earth and Planetary Science Letters 189, 269–276. doi:10.1016/S0012-821X(01)00367-3

Lowrie, W., Fuller, M., 1971. On the alternating field demagnetization characteristics of multidomain thermoremanent magnetization in magnetite. Journal of Geophysical Research. doi:10.1029/JB076i026p06339

McArthur, J M M, Crame, J.A., Thirlwall, M.F., 2000. Definition of Late Cretaceous stage boundaries in Antarctica using Sstrontium ssotope stratigraphy. The Journal of Geology 108, 623–640. doi:10.1086/317952

McFadden, P.L., McElhinny, M.W., 1988. The combined analysis of remagnetization circles and direct observations in palaeomagnetism. Earth and Planetary Science Letters 87, 161–172. doi:10.1016/0012-821X(88)90072-6

McFadden, P.L., McElhinny, M.W., 1990. Classification of the reversal test in palaeomagnetism. Geophysical Journal International 103, 725–729.

Medina, F.A., Buatois, L.A., 1992. Bioestratigrafia del Aptiano–Campaniano (Cretacico superior) en la Isla James Ross, in: Rinaldi, C.A. (Ed.), Geologia de La Isla James Ross. Instituto Antartico Argentino, Buenos Aires. Instituto Antártico Argentino, Buenos Aires, pp. 7–36.

Milanese, F.N., Olivero, E.B., Kirschvink, J.L., Rapalini, A.E., 2017. Magnetostratigraphy of the Rabot Formation, Upper Cretaceous, James Ross Basin, Antarctic Peninsula. Cretaceous Research 72, 172–187. doi:10.1016/j.cretres.2016.12.016

Milanese, F.N., Olivero, E.B., Raffi, M.E., Franceschinis, P.R., Gallo, L.C., Skinner, S.M., Mitchell, R.N., Kirschvink, J.L., Rapalini, A.E., 2019a. Mid Campanian-Lower Maastrichtian magnetostratigraphy of the James Ross Basin, Antarctica: Chronostratigraphical implications. Basin Research 31, 562–583. doi:10.1111/bre.12334

Milanese, F.N., Rapalini, A.E., Slotznick, S.P., Tobin, T.S., Kirschvink, J.L., Olivero, E.B., 2019b. Late Cretaceous paleogeography of the Antarctic Peninsula: New paleomagnetic pole from the James Ross Basin. Journal of South American Earth Sciences 91, 131–143. doi:10.1016/j.jsames.2019.01.012

Montes, M., Beamut, E., Nozal, F., Santillana, S.N., 2019. Late Maastrichtian-Paleocene chronostratigraphy from Seymour Island (James Ross Basin, Antarctic Peninsula): Eustatic controls on sedimentation. Advances in Polar Science 30, 303-327.

Montgomery, P., Hailwood, E.A., Gale, A.S., Burnett, J.A., 1998. The magnetostratigraphy of Coniacian-Late Campanian chalk sequences in southern England. Earth and Planetary Science Letters 156, 209–224. doi:http://dx.doi.org/10.1016/S0012-821X(98)00008-9

Nagy, L., Williams, W., Muxworthy, A.R., Fabian, K., Almeida, T.P., Conbhuí, P.Ó., Shcherbakov, V.P., 2017. Stability of equidimensional pseudo–single-domain magnetite over billion-year timescales. Proceedings of the National Academy of Sciences 114, 10356–10360. doi:10.1073/pnas.1708344114

Ogg, J.G., Ogg, G.M., Gradstein, F.M., 2016. A Concise Geologic Time Scale:

2016. Elsevier B.V., Amsterdam, Oxford, Cambridge, 234 pp.

Olivero, E.B., 1992. Asociaciones de Amonites de la Formación Santa Marta (Cretácico Tardío), Isla James Ross, Antártida, in: Rinaldi, C.A. (Ed.), Geología de La Isla James Ross. Instituto Antártico Argentino, Buenos Aires, pp. 45–75.

Olivero, E.B., 2012a. Sedimentary cycles, ammonite diversity and palaeoenvironmental changes in the Upper Cretaceous Marambio Group, Antarctica. Cretaceous Research 34, 348–366. doi:10.1016/j.cretres.2011.11.015

Olivero, E.B., 2012b. New Campanian kossmaticeratid ammonites from the James Ross Basin, Antarctica, and their possible relationships with Jimboiceras? antarcticum Riccardi. Revue de Paleobiologie 31, 133–149. doi:10.1016/j.cretres.2011.11.015

Olivero, E.B., Medina, F., 2000. Patterns of Late Cretaceous ammonite biogeography in southern high latitudes: the family Kossmaticeratidae in Antarctica. Cretaceous Research 21, 269–279. doi:10.1006/cres.1999.0192

Olivero, E.B., Scasso, R.A., Rinaldi, C.A., 1986. Revision of the Marambio Group, James Ross Island, Antarctica. Contribución del Instituto Antártico Argentino 331, 27 pp.

Olivero, E.B., Ponce, J.J., Martinioni, D.R., 2008. Sedimentology and architecture of sharp-based tidal sandstones in the upper Marambio Group, Maastrichtian of Antarctica. Sedimentary Geology 210, 11–26.

doi:10.1016/j.sedgeo.2008.07.003

Pan, Y., Zhu, R., Banerjee, S.K., Gill, J., Williams, Q., 2000. Rock magnetic properties related to thermanl treatment of siderite: Behavior and interpretation. Journal of Geophysical Research 105, 783–794.

Petersen, S. V., Dutton, A., Lohmann, K.C., 2016. End-Cretaceous extinction in Antarctica linked to both Deccan volcanism and meteorite impact via climate change. Nature Communications 7, 1–9. doi:10.1038/ncomms12079

Poblete, F., Roperch, P., Arriagada, C., Ruffet, G., Ramírez de Arellano, C., Hervé, F., Poujol, M., 2016. Late Cretaceous–early Eocene counterclockwise rotation of the Fueguian Andes and evolution of the Patagonia–Antarctic Peninsula system. Tectonophysics 668–669, 15–34. doi:10.1016/j.tecto.2015.11.025

Raffi, M.E., Olivero, E.B., 2016. The ammonite genus Gaudryceras from the Santonian-Campanian of Antarctica: Systematics and biostratigraphy. Ameghiniana 53, 375–396. doi:10.5710/AMGH.29.02.2016.2972

Reguero, M., Goin, F.J., Hospitaleche, C.A., Marenssi, S.A., Dutra, T., 2013. Late Cretaceous/Paleogene West Antarctica Terrestrial Biota and its Intercontinental Affinities, in: Springer Briefs in Earth System Sciences. Springer, Dordrecht, pp. 19–25. doi:10.1007/978-94-007-5491-1_1

Roberts, E.M., Lamanna, M.C., Clarke, J.A., Meng, J., Gorscak, E., Sertich, J.J.W., O'Connor, P.M., Claeson, K.M., MacPhee, R.D.E., 2014. Stratigraphy and vertebrate paleoecology of Upper Cretaceous-? lowest

Paleogene strata on Vega Island, Antarctica. Palaeogeography, Palaeoclimatology, Palaeoecology 402, 55–72. doi:10.1016/j.palaeo.2014.03.005

Scasso, R.A., Olivero, E.B., Buatois, L.A., 1991. Lithofacies, biofacies, and ichnoassemblage evolution of a shallow submarine volcaniclastic fan-shelf depositional system (Upper Cretaceous, James Ross Island, Antarctica). Journal of South American Earth Sciences 4, 239–260. doi:10.1016/0895-9811(91)90034-I

Tobin, T.S., 2017. Recognition of a likely two-phased extinction at the K-Pg boundary in Antarctica. Scientific Reports 7, 1–11. doi:10.1038/s41598-017-16515-x

Tobin, T.S., Ward, P.D., Steig, E.J., Olivero, E.B., Hilburn, I.A., Mitchell, R.N., Diamond, M.R., Raub, T.D., Kirschvink, J.L., 2012. Extinction patterns, δ 18 O trends, and magnetostratigraphy from a southern high-latitude Cretaceous–Paleogene section: links with Deccan volcanism. Palaeogeography, Palaeoclimatology, Palaeoecology 350–352, 180–188. doi:10.1016/j.palaeo.2012.06.029

Torres Carbonell, P.J., Dimieri, L. V, Olivero, E.B., Bohoyo, F., Galindo-Zaldívar, J., 2014. Structure and tectonic evolution of the Fuegian Andes (southernmost South America) in the framework of the Scotia Arc development. Global and Planetary Change 123, 174–188. doi:10.1016/j.gloplacha.2014.07.019

Vandamme, D., 1994. A new method to determine paleosecular variation.

Physics of the Earth and Planetary Interiors 85, 131–142. doi:10.1016/0031-9201(94)90012-4

Whitham, A.G., Ineson, J.R., Pirrie, D., 2006. Marine volcaniclastics of the Hidden Lake Formation (Coniacian) of James Ross Island, Antarctica: an enigmatic element in the history of a back-arc basin. Geological Society, London, Special Publications 258, 21–47. doi:10.1144/GSL.SP.2006.258.01.03

Wilson, T.J., 1991. Transition from back-arc to foreland basin development in the southernmost Andes: stratigraphic record from the Ultima Esperanza District, Chile. Geological Society of America Bulletin 103, 98–111. doi:10.1130/0016-7606(1991)103<0098:TFBATF>2.3.CO;2

Witts, J.D., Whittle, R.J., Wignall, P.B., Crame, J.A., Francis, J.E., Newton, R.J., Bowman, V.C., 2016. Macrofossil evidence for a rapid and severe Cretaceous-Paleogene mass extinction in Antarctica. Nature Communications 7, 1–8. doi:10.1038/ncomms11738

Tables and figures captions

Figure 1. Cretaceous-Paleogene units from Gustav and Marambio Groups. The black square in the inset indicates the location of the James Ross Basin with respect to the Antarctic Peninsula and the black dashed box indicates the study area (detailed in Figure 3). After Milanese *et al.* (2019a) and Olivero (2012a).

Figure 2. Chronostratigraphic scheme of the Marambio Group and upper Hidden Lake Formation. Magnetostratigraphy of the distal facies, located at southeast James Ross Basin, is summarized from previous studies (Milanese *et al.*, 2019a, 2017; Tobin *et al.*, 2012). Several authors have suggested ages for the proximal facies of the northwest area: (1) Barreda *et al.* (1999) and Kennedy *et al.* (2007) based on palynomorph and ammonite biostratigraphy, (2) Olivero (2012a) based on ammonite biostratigraphy, (3) Crame *et al.* (2006) and McArthur *et al.* (2000) based on $^{87}Sr/^{86}Sr$ chemostratigraphy. Reference polarity time scale from Ogg et al. (2016).

Figure 3. a) Geological map from northwest James Ross Island. Red lines indicate sections sampled for magnetostratigraphy. Cretaceous units dip to the southeast (Brandy Bay) and to southeast and north (Santa Marta Cove). Embedded in the lower right corner is the location of the Ulu Peninsula, Brandy Bay, and Santa Marta Cove areas in the James Ross Basin. b) Composite sedimentary column of the Hidden Lake, Santa Marta, and lower Snow Hill Island Formations. To the right of this section, the stratigraphic position of partial sections indicated in part a) are plotted. As. = Ammonite Assemblage. Both figures have been modified from Olivero (1992). We refer the reader to

Olivero (2012b), Olivero and Medina (2000) and Scasso et al. (1991) to check stratigraphic correlations.

Figure 4. Example slope corrected hysteresis loops (a), IRM/Backfield curves and IRM coercivity spectra (b) and Lowrie-Fuller tests (c) measured for samples from northwest James Ross Island. These analyses suggest the primary ferromagnetic carrier is in the titanomagnetite series and has vortex state/pseudo-single domain size. All analyses available in Figures S2, S3 and S4. IRM=isothermal remanent magnetization, ARM=anhysteric remanent magnetization, dIRM=IRM gradient, dField=Field gradient.

Figure 5. Paleomagnetic behaviors of samples from Hidden Lake Formation (a), Alpha Member (b), Beta Member (c) and Snow Hill Island Formation (d). In most cases, two directions were isolated: a small viscous component (marked in green in the orthographic projections) at the first demagnetization steps and a ChRM direction (marked in red) that decays straight to the origin until the ~ 500 °C. Paleomagnetic ChRM directions were isolated using principal component analysis in most samples. In some cases (*e.g.* 5b), ChRM direction was obtained by great circle analysis. A few cases with magnetization remaining above 550 °C (*e.g.* 5c) could indicate that hematite is probably also present in addition to magnetite. Blocking temperatures show a wide distribution, a common feature in sedimentary rocks. J=Magnetization, J_0=Initial magnetization.

Figure 6. Cretaceous northwest James Ross Island mean paleomagnetic directions on equal area plot in tilt-corrected coordinates. Main stereographic projection shows normal and reverse populations with their respective means. In the upper left, global mean direction with reverse components transposed to

the upper hemisphere. Empty (black) symbols for upper (lower) hemisphere in the stereographic projection. Detailed results are given in Table 1.

Figure 7. Paleomagnetic declination, inclination and interpreted polarities of partial sections from Ulu Peninsula Cretaceous units (see Fig. 3). Directions obtained by Principal Component Analysis (PCA; Kirschvink, 1980) are indicated with solid symbols and those obtained by Great Circle Analysis (McFadden and McElhinny, 1988) with empty ones. Declination goes from -90° to 270°, inclination from -90° to 90°, and virtual geomagnetic poles (VGP) latitude from 90° to -90°, from left to right. As.=Ammonite assemblages from Olivero (2012), M=Mud, S=Sand, G=Gravel. See supplementary material for magnetic declination, inclination and MAD of each section (Figs. S7 to S20).

Figure 8. Composite sedimentary column and paleomagnetic directions expressed as Virtual Geomagnetic Pole (VGP) latitude (°). Those VGPs with latitude > (<) 0° are interpreted of normal (reverse) polarity. The stripe centered at 0° is 20° wide and indicates samples considered as transitional according to the applied secular variation filter (Vandamme, 1994). To the right, interpreted polarity and the proposed correlation with the Global Polarity Time Scale from Ogg *et al.* (2016). As.=Ammonite assemblages from Olivero (2012a), M=Mud, S=Sand, G=Gravel. See supplementary material for paleomagnetic directions expressed as Declination and Inclination (Fig. S6).

Figure 9. Compilation of magnetostratigraphic results of the James Ross Basin. Northwest area represents the proximal facies of the sedimentary infill and its results are presented in this work. The southeast sector results from distal facies previously published by Milanese *et al.* (2017, 2018) in southeast James Ross Island and Snow Hill Island, and by Tobin *et al.* (2012) in Marambio

(Seymour) Island. Intra-basin correlation of sedimentary columns is based on C33R/C33N reversion and ammonite assemblages. Black magnetic polarities are normal, white are reverse and gray indicates transitional or ambiguous interpreted polarity. Reference polarity time scale is based on Ogg *et al.* (2016). Adapted from Olivero (2012a). As. = Assemblage.

Figure 10. Sedimentary accumulation rates for the Marambio Group, based on magnetosgratigraphy from Figure 9. GPTS is the Global Polarity Time Scale from Ogg et al. (2016).

Figure 11. Proposed chronostratigraphy for the Marambio Group and upper Hidden Lake Formation, integrating magnetostratigraphies from this work and Milanese *et al.* (2019a, 2017) and Tobin *et al.* (2012). Compared age frameworks from (1) Barreda *et al.* (1909) and Kennedy *et al.* (2007) based on palynomorph and ammonite biostratigraphy, (2) Olivero (2012a) based on ammonite biostratigraphy, (3) Crame *et al.* (2006) and McArthur *et al.* (2000) based on inoceramids and $^{87}Sr/^{86}Sr$ chemostratigraphy. Reference polarity time scale from Ogg et al. (2016). Sant. = Santonian; C. = Coniacian.

Table 1. Paleomagnetic means, reversal test values and paleopole coordinates for the Upper Cretaceous Marambio Group at northwest James Ross Island. These data also includes directions from the upper Hidden Lake Foration. Stratigraphic = tilt-corrected.

Paleomagnetic means for Cretaceous units from NW James Ross Basin

Paleomagnetic mean	**Dec (°)**	**Inc (°)**	**α95(°)**	**κ**	**N**
In situ	30.5	-74.8	3.8	9.9	158
Stratigraphic	2.7	-71.3	3.9	9.4	158
Normal strat. mean	8.8	-69.2	4.2	10.3	124
Reverse strat. mean	146.6	76.2	9.2	8.2	34

Reversal test from stratigraphic means	**Critical Angle (°)**	**Observed Angle (°)**	**Condition**
	15.1	13.9	Positive (Class C)

Paleomagnetic pole	**Lat (°)**	**Long (°)**	**A95**	**Age**
	-82.7	134.2	6.1	*ca.* 80 Ma

Highlights

- The Santonian-Campanian boundary has been precisely determined in Antarctica.
- A new chronostratigraphical framework for the James Ross Basin is presented.
- The correlation of proximal and distal facies is based on C33R/C33N limit.
- The Coniacian-Santonian boundary has been inferred within the Hidden Lake Formation.